
Article:
Wang, T.-H., Huang, Y. and Park, J. (2022) Development of daylight glare analysis method using an integrated parametric modelling approach: a comparative study of glare evaluation standards. Buildings, 12 (11). 1810. ISSN 2075-5309

https://doi.org/10.3390/buildings12111810

---

buildings

MDPI

Article

Development of Daylight Glare Analysis Method Using an Integrated Parametric Modelling Approach: A Comparative Study of Glare Evaluation Standards

Tsung-Hsien Wang [1], Yichun Huang [2] and Jihyun Park [3,*]

[1] School of Architecture, University of Sheffield, Sheffield S10 2TN, UK
[2] Surbana Jurong Private Limited, Shanghai 200082, China
[3] Department of Architecture, Ewha Womans University, Seoul 03760, Korea
* Correspondence: jh.park@ewha.ac.kr

Abstract: Conducting lighting simulations to investigate lighting performance, such as glare, is widely accepted and of particular interest in the design development stage. However, the main challenge remains in integrating lighting performance metrics into a streamlined modelling and evaluation workflow. With the advancement in digital and modelling technologies, an automatic workflow of modelling parametric design studies with lighting performance evaluation becomes feasible. This study investigates a parametric modelling approach to facilitate glare evaluation using China Green Building Standard as an example. Their glare evaluation adopted the known daylight glare index (DGI) with a revised glare source definition in the calculation. An evaluation toolkit is presented, demonstrating its applications with the sky model. Compared with DGI, the results articulate how a parametric modelling workflow can automate lighting performance evaluation and facilitate technical investigation and clarifications for glare evaluation. Through the parametric simulation studies, the differences in the limited metric scale and the sensitivity of capturing window sizes on the glare evaluation suggest future evaluation protocols for the environmental standard development.

Keywords: lighting; daylight; glare; DGI; DGI in China; lighting simulation; parametric modeling workflow; green building standards

Citation: Wang, T.-H.; Huang, Y.; Park, J. Development of Daylight Glare Analysis Method Using an Integrated Parametric Modelling Approach: A Comparative Study of Glare Evaluation Standards. *Buildings* **2022**, *12*, 1810. https://doi.org/10.3390/buildings12111810

Academic Editor: Danny Hin Wa Li

Received: 7 September 2022
Accepted: 24 October 2022
Published: 28 October 2022

1. Introduction

Lighting is one of the essential factors, including energy, air, and acoustic, contributing to holistic indoor environmental quality (IEQ). While considering daylighting in buildings for energy savings, health, and well-being, contemporary building design with glass facades could lead to excessive solar gains and visual discomfort [1]. To evaluate the lighting quality of an indoor environment, illuminance and luminance-based approaches are taken to examine visual impacts from daylighting or artificial lighting. Measuring illuminance or luminance levels in the indoor environment is the first step to evaluating the visual impacts of lighting sources and serves as the basis for investigating the occupants' visual comfort [2,3].

Green building standards often stipulate thresholds as the design guidelines to ensure lighting quality indoors [4–6]. Specifically, for glare evaluation, the prevailing approach considers the glare source luminance, size, relative positions of glare sources within the field of view, and the overall background luminance or illuminance [7,8]. Metrics, saturation-based (overall illuminance on the eye) or contrast-based (luminance ratio in the field of view), are commonly employed to evaluate lighting intensity in the indoor environment [9]. Such evaluation ensures that suitable lighting levels are provided for intended indoor tasks while meeting prescribed requirements from chosen governing standards.

Glare is subjective to personal perception and varies enormously from person to person [10,11]. Within the field of view, direct luminaires can lead to visual discomfort.

Numerous efforts have been made to quantify this condition since the 1950s [1,12]. When assessing glare in the indoor environment, the essential parameters include (1) the glare size (e.g., the size of the window), (2) the glare source luminance (L_g), (3) the relative glare source location from the viewer, and (4) the background luminance (L_b) of the view [13]. Causes of glare in indoor spaces include exterior windows that allow excessive daylight, high-illuminance lighting, direct light to the space where users usually stay or the screen, or indoor environments that reflect light from the window. Although the degree of discomfort or perception felt by each person may differ, it can still be quantified by the abovementioned elements. Data associated with these parameters could also be collected from on-site field measurements, and alternatively, computer-based lighting simulations could be used [10,14]. While considering daylight during the conceptual building design phase, only simulation will be available and used primarily to guide indoor lighting design and assess lighting quality against prescribed thresholds in selected country standards.

Good lighting conditions have been considered for high-performance building design in recent years. In contemporary offices, people often share spaces and spend a long time indoors. Visual comfort, among others, is unquestionably critical and essential for enhanced health, well-being, and productivity [15–17]. To ensure the visual comfort and satisfaction of building users, glare is an essential element to be considered in building design [18]. Looking at the glare evaluation from international green building standards, LEED by USGBC [19] considers disability glare in new construction by setting an upper limit on illuminance levels for daylight environments. In WELL by IWBI [20], all glazing should be less than 2.1 m above the floor in regularly occupied spaces and satisfy at least one of three criteria: (1) interior window shading or blinds that are controllable by the occupants or set to automatically prevent glare, (2) external shading systems that are set to prevent glare, (3) variable opacity glazing, such as electrochromic glass, which can reduce transmissivity by 90% or more. BREEAM BRE [21] includes surrounding buildings, structures or other permanent environmental features when using simulation modelling to assess the risk of glare for both direct sunlight and reflected glare from glazing or reflective surfaces. In China, green building (GB) standards also prescribe glare assessments to ensure indoor lighting quality when designing workplaces. For instance, GB/T50378-2019 [22] in China mainly includes six sections: safety and durability, health and comfort, occupant convenience, resources saving, environment livability, promotion, and innovation. The health and comfort section includes four environmental quality categories: indoor air quality, water quality, sound and daylighting, and indoor thermal environment. Among these categories, the sound and daylighting section stipulates the assessment of daylighting design and sunlight glare control.

1.1. Glare Assessment and Computation

A number of established glare indices were proposed and adopted worldwide, as summarized in Table 1. While some indices consider the same four fundamental parameters mentioned above, they are composed differently in various metrics using different exponents and constants to afford a common computational basis. DGI [23,24] and DGP [25] are suitable for evaluating daylighting. Others, such as UGR [26], VCP [27–30], and DGR [26], are for assessing artificial lighting conditions with small sources.

Table 1. Glare indices with required parameters.

Glare Index	Requires Parameters	Glare Source	References
BGI—British Glare Index	L_s, L_b, $W_{(sr)}$, P_s	Small Source	[31]
DGI—Daylight Glare Index	L_s, L_b, $W_{(sr)}$, P_s	Artificial and Nature lighting; Small Source	[23,24,32]
CGI—CIE Glare Index	L_s, $W_{(sr)}$, P_s	Small Source	[33]
DGP—Daylight Glare Probability	L_s, E_v, $W_{(sr)}$, P_s	Natural lighting; Large and Small	[25]
UGR—Unified Glare Rating	L_s, L_b, $W_{(sr)}$, P_s	Artificial lighting; Small Source	[26]
VCP—Visual Comfort Probability	L_s, L_b, $W_{(sr)}$, P_s	Artificial lighting; Small Source	[27–30]
DGR—Discomfort Glare Rating	L_s, L_b, $W_{(sr)}$, P_s	Artificial lighting; Small Source	[26]

L_s: Glare Source Luminance, L_b: Background Luminance, E_v: is the vertical eye illuminance, $W_{(sr)}$: Solid angle formed by the glare source(s), P_s: Viewing Position.

The essential step of evaluating glare mentioned above starts by defining what constitutes a glare source in a complex environment and, in particular, how this factor is calculated in the function associated with its limitations and applicable areas. The prevailing methods for glare source detection include (1) a fixed threshold value, (2) a calculated threshold based on the background scene luminance, and (3) a calculated threshold associated with the task luminance. The choice of the threshold method will significantly influence the reliability of the glare evaluation [8].

1.2. Evaluating DGI and DGI in China

When evaluating DGI, a high dynamic range (HDR) image representing the field of view is often required. It can usually be provided using a suitable camera kit with a fish-eye lens or by conducting a lighting simulation [18,34,35]. Given an HDR image, a series of steps associated with image processing is then taken to evaluate glare source sizes, luminance and relative position indexes to the viewing location. Essential variables for glare evaluation could be computed with existing software tools, such as Radiance. According to Pierson et al. [8], the first step of identifying glare sources is based on the luminance level above the chosen threshold, e.g., several times the average background luminance. Identification of the intended glare conditions serves as an essential indicator for selecting a suitable threshold method and, thus, the applicability of the glare assessment [36].

In the China green building standard, local experiments suggested that the climatic conditions would result in glare conditions over 90% of the time if windows are too large [37]. The prevalent Daylight Glare Index (DGI) proposed initially by Hopkinson [24] is modified and included in the China national standard "GB 50033-2013 Standard for Daylighting Design of Buildings". The prescribed glare calculation is provided in Appendix B in GB 50033-2013 [37] and continues as applicable without changes in the new standard GB/T 50378-2019 [22], published in 2019. As discussed by Huang and Wang [38], the glare assessment in GB 50033-2013 used the original DGI function yet changed the definition of one parameter, L_s, the glare source luminance in the original function proposed by Hopkinson. In the prescribed DGI evaluation in China (DGI_{China}), the glare source is now defined differently to use the entire source's average brightness, namely the whole window, instead of using sections of sources that have brightness above a specific multitude of adaptation levels. The modified DGI calculation is summarized below,

$$DGI(China) = 10 \log \sum G_n \tag{1}$$

where glare constant for each external window G_n in the room is:

$$G_n = 0.48 \frac{L_s^{1.6} \Omega^{0.8}}{L_b + 0.07 \omega^{0.5} L_s} \tag{2}$$

G_n = glare constant;
L_s = window brightness, the weighted average luminance of sky, shading objects and ground through window (cd/m^2);
L_b = average background luminance, resulting from all visible internal surfaces (cd/m^2);
ω = solid angle formed by the window against the calculation point (sr);
Ω = solid angle with window position correction considered (sr).

The definition of Ω (solid angle subtended by each window modified by position index) also follows prevalent glare metrics:

$$\Omega = \int \frac{d\omega}{p^2} \tag{3}$$

where p is Guth position index:

$$p = exp[(35.2 - 0.31889\alpha - 1.22e^{-\frac{2\alpha}{9}})10^{-3}\beta + (21 + 0.26667\alpha - 0.002963\alpha^2)10^{-5}\beta^2] \quad (4)$$

where

α = angle from vertical axis to center of window;
β = angle between view axis and center of window.

The second modification in DGI_{China} is the acceptable threshold value, but it does not affect computation and is thus less of a concern in the modelling and calculation processes. "Daylighting Grade" is a classification used in the China standard, and, for example, offices and conference rooms have a Grade-III requirement, whereas copy rooms have a Grade-IV requirement. While corresponding notional window brightness is listed in Table 2, these values are for reference only since the standard uses calculated DGI_{China} values for evaluation. Table 2 illustrates Daylighting Grade with associated DGI_{China} threshold values and equivalent DGI values in UK standards.

Table 2. Daylighting Grade in China Standard GB 50033-2013.

Daylighting Grade	Level of Glare Perception	Window Brightness (cd/m^2)	DGI_{China}	DGI (UK)
I	No glare	2000	20	19
II	Slight Perception	4000	23	22
III	Acceptable	6000	25	24
IV	Discomfort	7000	27	26
V	Intolerable	8000	28	28

This modification of the glare source definition in DGI_{China} results in difficulty when using current software tools to evaluate the new metric proposed in GB 50033-2013 [37]. For instance, using an HDR image solely will be challenging to distinguish a group of pixels representing a window area within a complex background combining sky conditions, shading objects, neighboring buildings, and ground through a window. To facilitate DGI_{China} evaluation, Huang and Wang [38] presented a standard alone software tool taking a Radiance simulation result file in the HDR format with an associated gbXML model initially prepared for the simulation. This stand-alone tool is sufficient in supporting evaluating DGI in China. However, incorporating such a tool into the iterative design process is still limited. For instance, getting instant feedback on how proposed new lighting design strategies would perform against the stipulated lighting thresholds would be desired and compels a need for concurrent glare evaluation. In this paper, we propose an integrated computational workflow incorporating the change prescribed in DGI_{China} and implementing the glare evaluation utility functions to facilitate GB 50033-2013 Glare assessment. The hypothesis is that the ease of operating lighting design compliance checks against the prevailing green building standard in China would fill the existing technology gap and increase the tool's adoption and impact on sustainable design practice. With the integrated computational assessment, this paper demonstrates the comparative study of DGI and DGI_{China} to uncover the significant differences and implications induced by the change in the glare source definition for daylight glare evaluation in China.

2. The Integrated Parametric Modelling Workflow

Prevalent Glare Metric Computation Workflow and Tools

The typical workflow for evaluating glare, including DGI, utilizes a three-stage process centered around lighting simulation. The first stage involves building geometry construction with material information specifications required for lighting simulation software. Radiance is the prevalent software used in industry, and it utilizes a text-based input

describing three-dimensional information of scene geometry and associated material properties. In the second stage, a lighting simulation is conducted to predict point luminance values in the scene. Radiance conducts stochastic backwards ray tracing to produce a bitmap image of the specified view with calculated luminance values for pixels [39]. These two stages are well-supported by current modelling tools and only require minimum user effort to prepare suitable building geometry for the simulation. The simulation results are then rendered as specified glare-view luminance-based images (hereafter referred to as Radiance images).

The third stage is to calculate glare metrics. In the case of common international glare metrics, such as VCP, UGR, and DGI, Radiance provides easy-to-use auxiliary programs to obtain the metrics from the simulation results in the form of Radiance images. These metrics usually define glare sources as areas within views having brightness above several times of background luminance (typically five times brighter). The Radiance images can, therefore, easily be used in a two-pass method [40]. The auxiliary program *findglare* parses the image to tabulate the average luminance of the image and finds regions that are too bright and considered glare sources (together with view directions, solid angles, and luminance of these glare sources). A second program *glarendx* uses the tabulated results to obtain the desired glare metric. These two programs are similarly easy to use and have facilitated the inclusion and use of glare metrics in the industry. Figure 1 illustrates the workflow from modeling and simulation to glare evaluation.

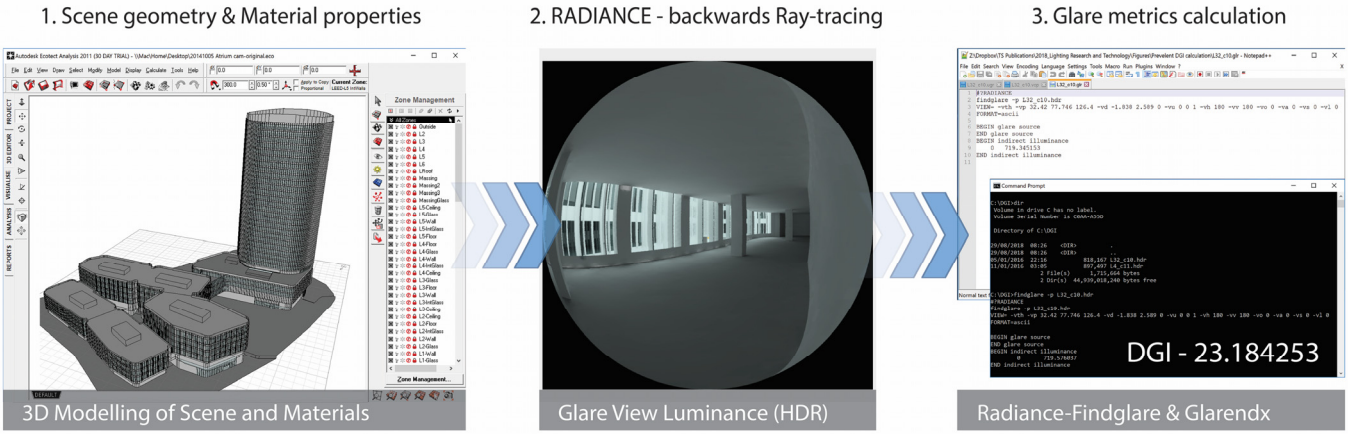

Figure 1. Prevalent 3-stage process to calculating common glare metrics via thresholding algorithms.

However, the variation introduced by DGI_{China} changes the glare source definition (L_s in Equation (2)). Since it is possible that a window might contain both sections brighter than the threshold as well as sections darker than the threshold luminance at the same time, it is no longer straightforward to use thresholding algorithms. Calculating DGI_{China} would, therefore, require minimally a Radiance image and the associated geometric information, which is not directly retrievable from the Radiance image. As a result, existing software programs, such as Radiance auxiliary program-*findglare*, are no longer applicable. As such, the automation of the DGI_{China} calculation necessitates a new computational workflow which incorporates both a Radiance image and an associated geometric model describing surface attributes for glare calculation. Huang and Wang [38] presented a stand-alone software tool demonstrating how DGI_{China} calculation can be automated given a Radiance image and the associated building information model in the gbXML format, as shown in Figure 2.

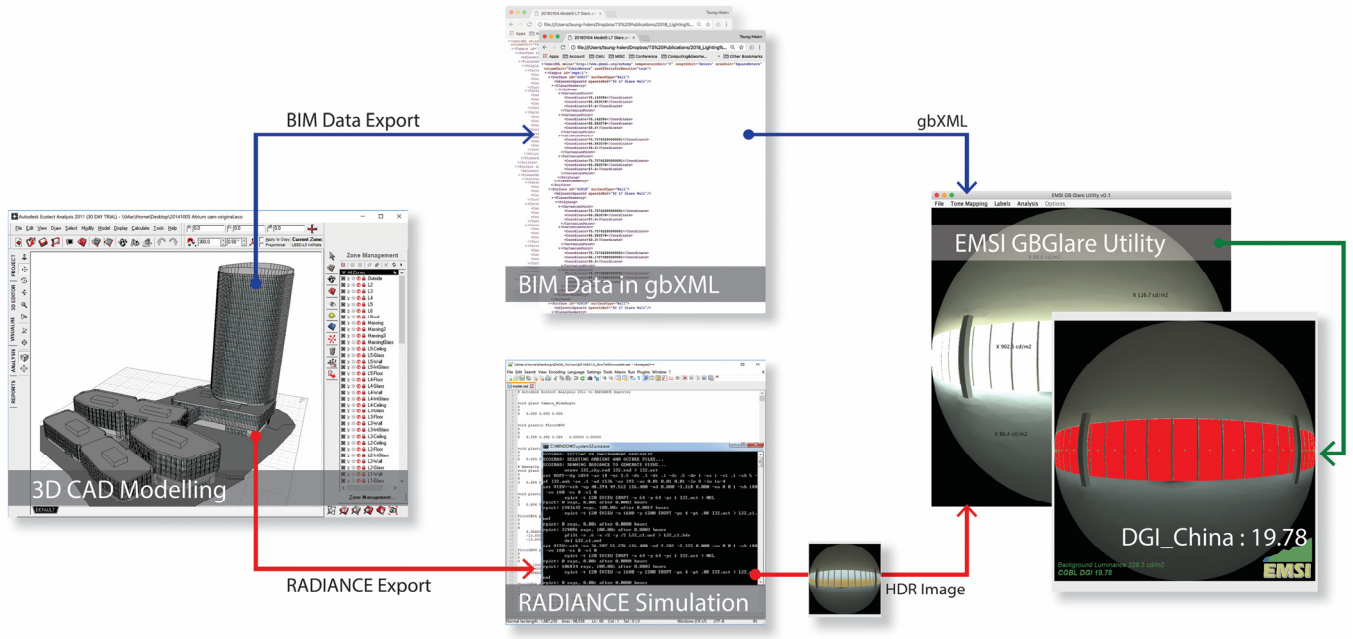

Figure 2. The stand-alone GBGlare Utility tool for calculating DGI_{China} using a HDR image with the associated building information model.

3. A Parametric Modelling Workflow to Enable DGI Evaluation during the Iterative Design Process

While considering glare assessments for designers during the iterative design process, a streamlined process from modelling, simulation to glare evaluation will be needed to afford instant feedback on design changes. In this paper, we further investigate how DGI_{China} can be calculated and evaluated in a computational design workflow combining parametric modelling, Radiance simulation, and glare assessments. To facilitate the development, we use a parametric modelling platform, Grasshopper3D for Rhinoceros 3D and develop glare evaluation toolkits for DGI_{China}. The computational workflow consists of three major steps, including (1) model preparation, (2) Radiance simulation, and (3) glare analysis, as shown in Figure 3. Step one includes preparing the surface geometry, material properties, viewing location and direction and weather information for the sky model generation. Step two executes the command-line function to run the Radiance simulation and retrieves the results. Step three computes selected glare indices, including DGI, DGI_{China} and DGP. Figure 4 illustrates the implementation combining existing components available in Grasshopper3D and customized DGI_{China} toolkits to automate daylight glare evaluation in China. The objective is to afford such performance-based evaluation in the parametric design workflow with minimum effort. As such, designers can better understand how their proposed building design performs during the iterative design process and explore how these evaluation results can be considered to inform further design decisions.

3.1. DGI Evaluation Toolkit Development

In this paper, we developed DGI Evaluation toolkits to facilitate daylight glare evaluation in China and, in particular, to manage required geometric information from a raw parametric model. For instance, data regarding surface types and materials are maintained for Radiance and window detection using raytracing to identify pixels for a window from an input Radiance image.

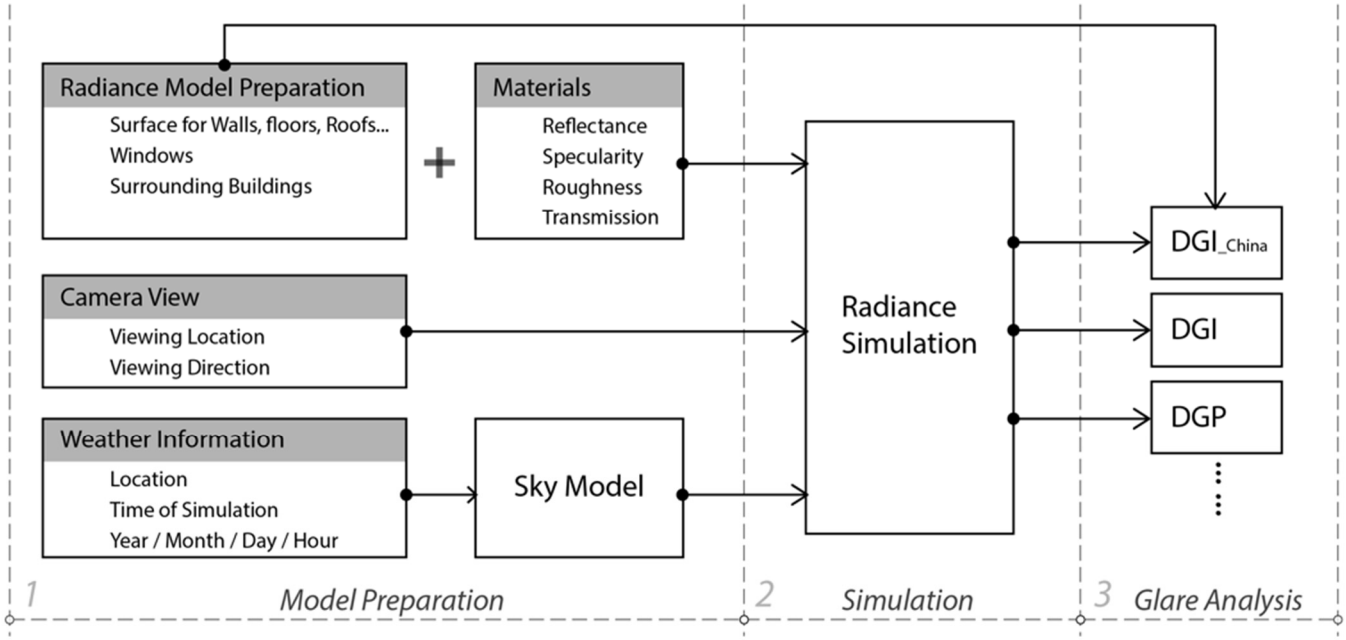

Figure 3. The computational workflow for the integration from the model preparation to glare analysis.

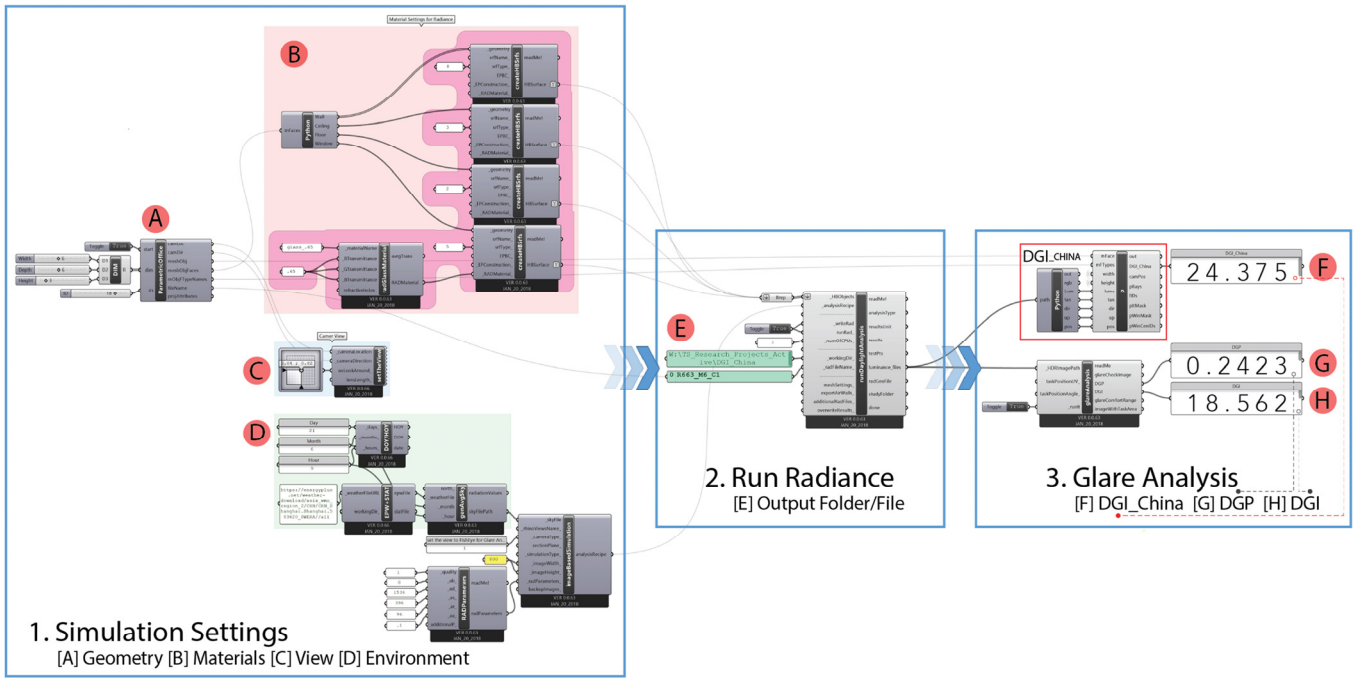

Figure 4. The computational procedure implemented in Grasshopper3D.

The development of DGI Evaluation toolkits consists of two major parts. The first part includes functions that decode a Radiance image to retrieve (1) viewing attributes such as the location and direction and (2) pixel luminance values, for which a scanline method is used to process each pixel in the image. The second part of the DGI_{China} calculation integrates the model surface attributes, namely the surface types, for backwards image-based raytracing. In this subprocess, the directional vector derived from each pixel is first obtained and then raytraced using mesh utility functions from Rhinocommon. Pixel-based sampling is then used to determine the number of pixels in the Radiance image constituting the actual window (as measured by steradians subtended from all visible windows). Since the image is a hemispherical projection defined as having 2π steradians, the solid angles of

the visible sections of windows are calculated as a ratio of the number of pixels representing windows over the pixels of the field of view. Figure 5 illustrates the evaluation workflow considering pixel locations, pixel luminance values, and surface geometry data to compute all components needed in DGI_{China}.

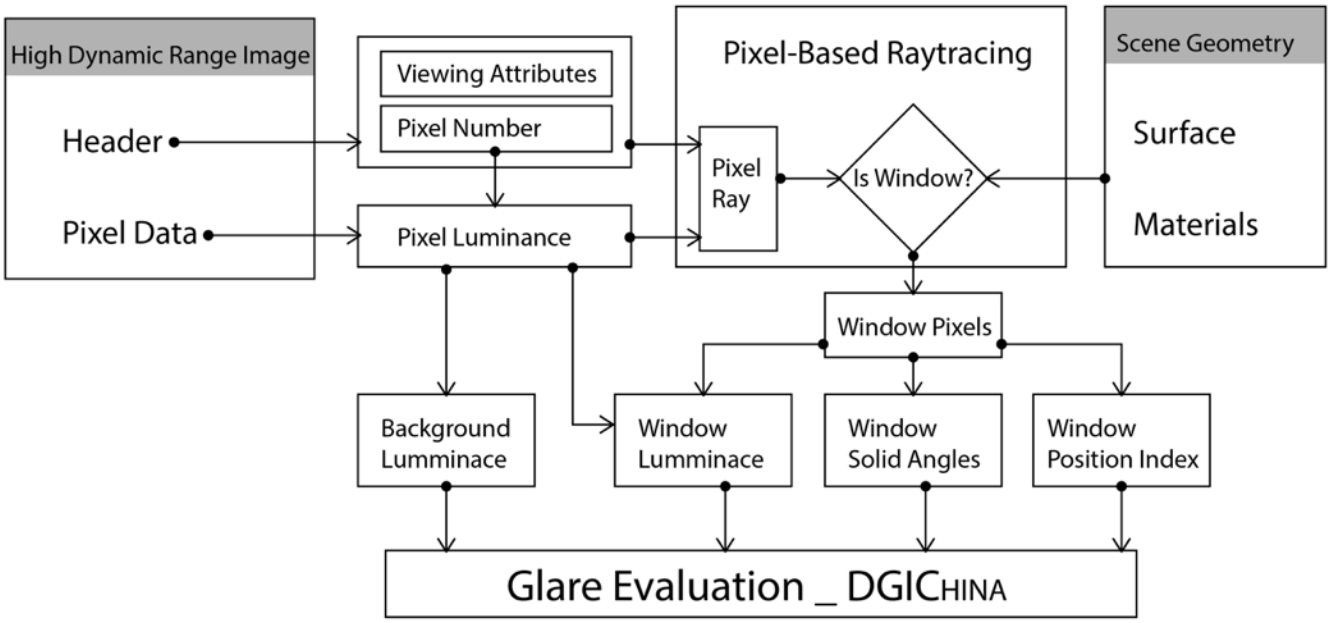

Figure 5. The DGI Evaluation workflow.

To summarize, the DGI_{China} toolkit seamlessly integrates DGI_{China} assessments into a computational modelling workflow and affords further parametric studies in a relatively straightforward fashion. By automating DGI_{China} in a parametric modelling workflow, hundreds, or thousands, of parametric permutations could be examined effortlessly, and this will allow designers to investigate optimal design solutions with the added consideration of glare evaluation. In the following, we demonstrate the applicability of this parametric modelling workflow through a conceptual case study evaluation to facilitate comparative investigation and clarifications for DGI_{China}.

3.2. Demonstration

The China standard for daylighting includes a protocol for a sky model to be used in daylighting (but not glare) simulation: a cloudy sky model with one of five stipulated specific horizontal illuminances according to geographical location. The standard establishes thresholds and sky models for daylighting based on actual weather data and simulation analysis. In this paper, we choose Shanghai as the geographical location for the case study and use the following three sky models, a cloudy model of 13,500 lx, a cloudy model of 35,000 lx, and the Shanghai sky model from the EnergyPlus weather database. We aim to include these three sky models to cover low, high, and dynamic sky conditions through selected simulation periods.

The chosen conceptual design case is a typical office space that could be easily found in China with a room width of 12-m, depth of 8-m and height of 3.2-m. As shown in Figure 6, this room has a south-facing window with a total of 25 parametric variations combining five window-wall width-ratio (WWR) and five window height (WinH) values. WWR value ranges from 0.5 to 0.9 with an incremental step of 0.1, and WinH value ranges from 0.6 m to 1.8 m with an incremental step of 0.3 m.

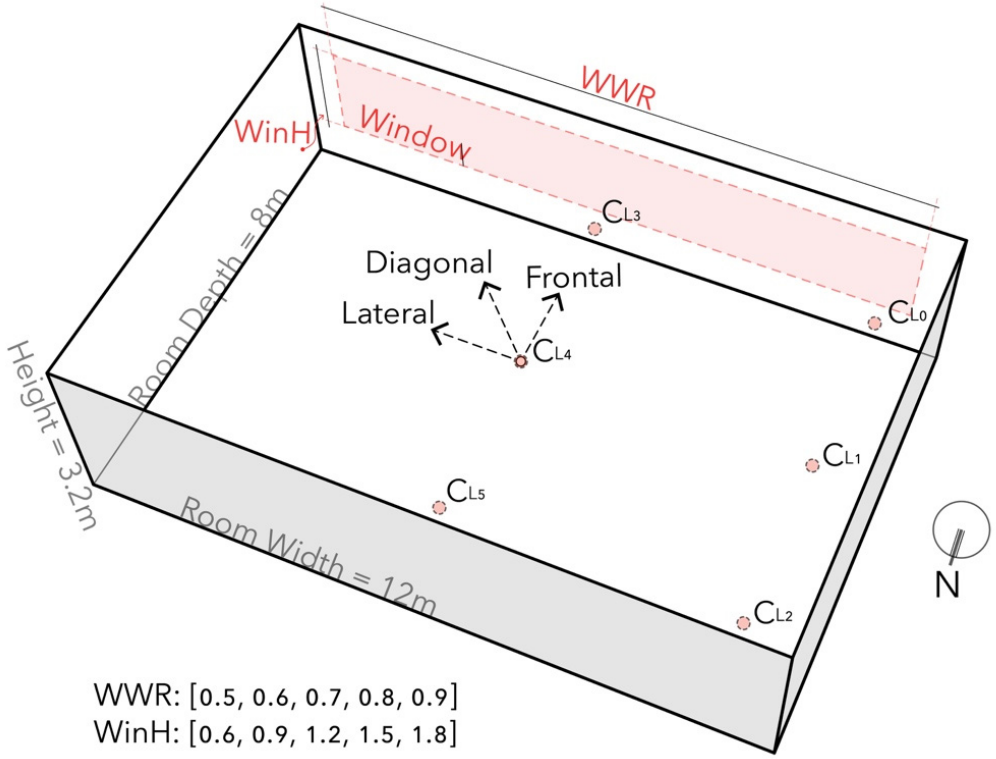

Figure 6. Parametric modelling workflow case study and viewing positions. WWH: Window Width Ratio and WinH: Window Height (meter).

In addition to twenty-five variations in the window dimension, we consider six different camera locations with three viewing directions. As shown in Figure 6, camera locations are evenly distributed at the near, middle, and far locations with respect to the window opening along the west side of the room (CL_0, CL_1, CL_2) and the north-central axis (CL_3, CL_4, CL_5). We choose only the west side of the room as the representative to cover the symmetrical counterpart. For the calculation, three viewing directions cover frontal, lateral and diagonal viewing angles per camera location. The height of the camera location is 1.7 m in this project. Together with camera locations, viewing angles, and parametric geometry variations, we generate a total of 1350 glare calculations, combining 5(WWR) $\times$ 5(WinH) $\times$ 6(C_{Loc}) $\times$ 3(V_{Dir}) $\times$ 3(WEP).

3.3. Comparative Study

Through this case study, we aim to examine the DGI_{China} simulation results and discuss the findings by comparing them with the prevailing glare index—DGI. The objective is to understand the implications induced by the change in the glare source definition introduced in DGI_{China}. Together with twenty-five window variations, six camera locations and three viewing angles, we generate a total of 450 cases per sky model. As discussed above, we use two China standard sky models with an average of 13,500 lx and 35,000 lx luminance and one additional sky model from the EnergyPlus Weather database for Shanghai. We first examine sky models' impacts on DGI and DGI_{China} evaluation. As shown in Figure 7, a total of six groups of simulation results were analyzed. Among the three sky models used in the simulation, the sky model of 13,500 lx is the darkest and EnergyPlus weather for Shanghai (EPW) has the average highest luminance. We analyze the statistical difference between DGI and DGI_{China} values.

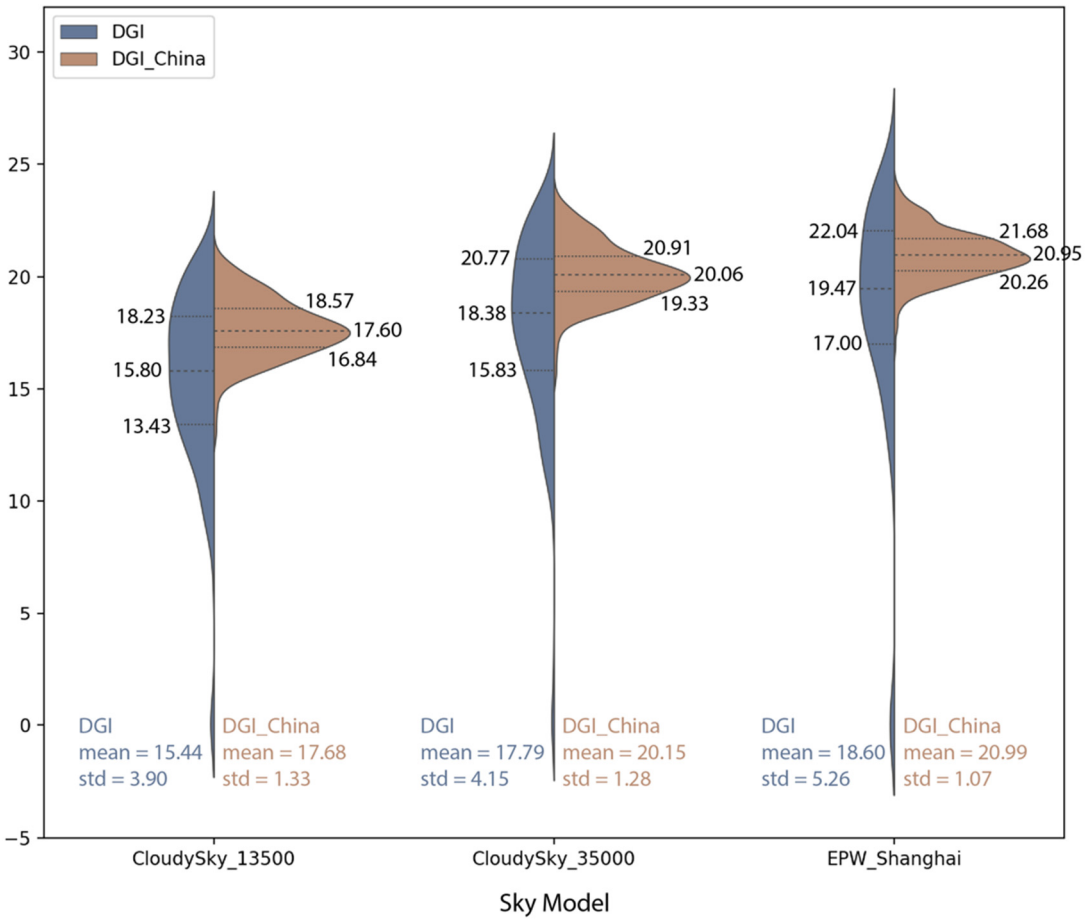

Figure 7. Comparison of Sky models on DGI and DGI_{China}.

3.3.1. Sky Models

Overall, DGI_{China} shows less variation across three sky models than DGI yet shares similar trends. Both DGI_{China} and DGI show a positive correlation with sky model luminance. However, we note from the data, both in generality and by sky type, that the range of computed DGI_{China} is relatively limited for a typical China office design. The resulting variation is less than 3 on the scale, whereas DGI has an average above 5. We also find that most of the calculated DGI_{China} values are well below the slight perception threshold (<22). This result sustains the indication that the DGI_{China} metric has insufficient sensitivity, as discussed by Huang and Wang [38]. As a result, the defined scale and thresholds would require further examination.

3.3.2. Impacts from Sky Models on DGI and DGI_{China}

We further analyze the evaluation results by grouping them with camera locations and viewing directions. Figure 8 shows the results for the front viewing location closest to the window, Figure 9 for the middle locations along the viewing axis, and Figure 10 for the far viewing locations. In total, there are 18 camera viewing groups. DGI results were plotted with a solid line pattern shaded in blue and DGI_{China} in a solid line pattern shaded in orange. We note that the viewing groups closest to the window in the front show a significant deviation between DGI and DGI_{China}. Among six front camera viewing locations, all DGI values start to decrease once the glare source size amounts to 0.8 and above in steradian. In contrast, DGI_{China} continues increasing gently, as shown in Figure 8. Among a total of 18 viewing positions, DGI_{China} evaluation consistently correlates positively with the glare source size (measured in steradian).

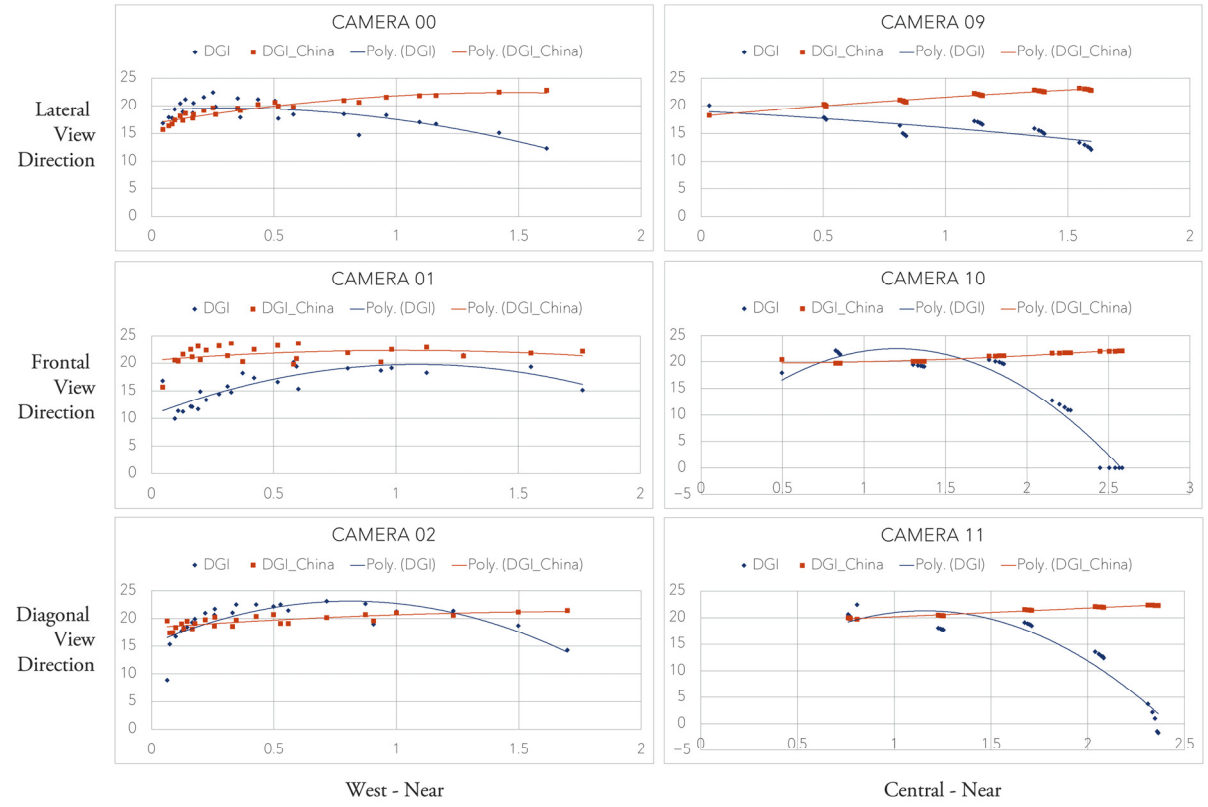

Figure 8. Comparative study on camera viewing location near the window with solid angles (*X*-axis) against DGI and DGI_{China} evaluation (*Y*-axis).

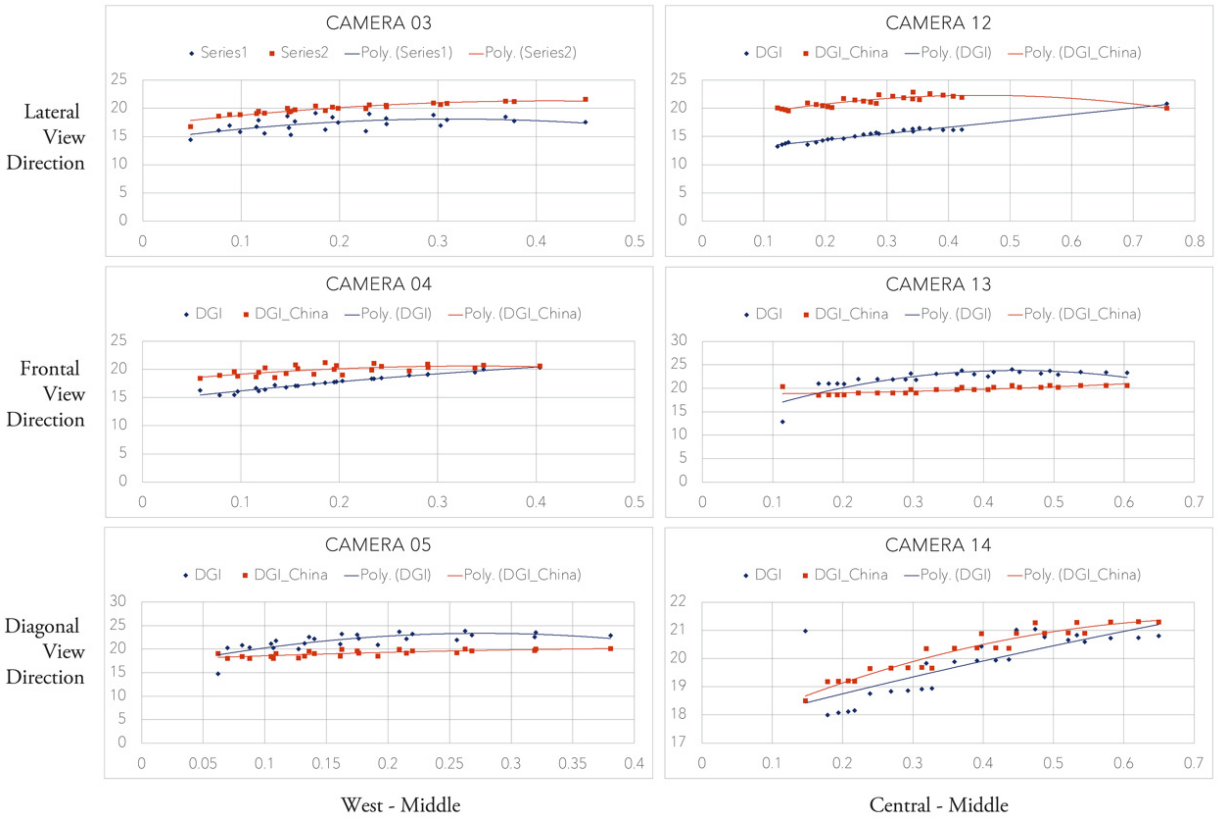

Figure 9. Comparative study on camera viewing location at the center of the room with solid angles (*X*-axis) against DGI and DGI_{China} evaluation (*Y*-axis).

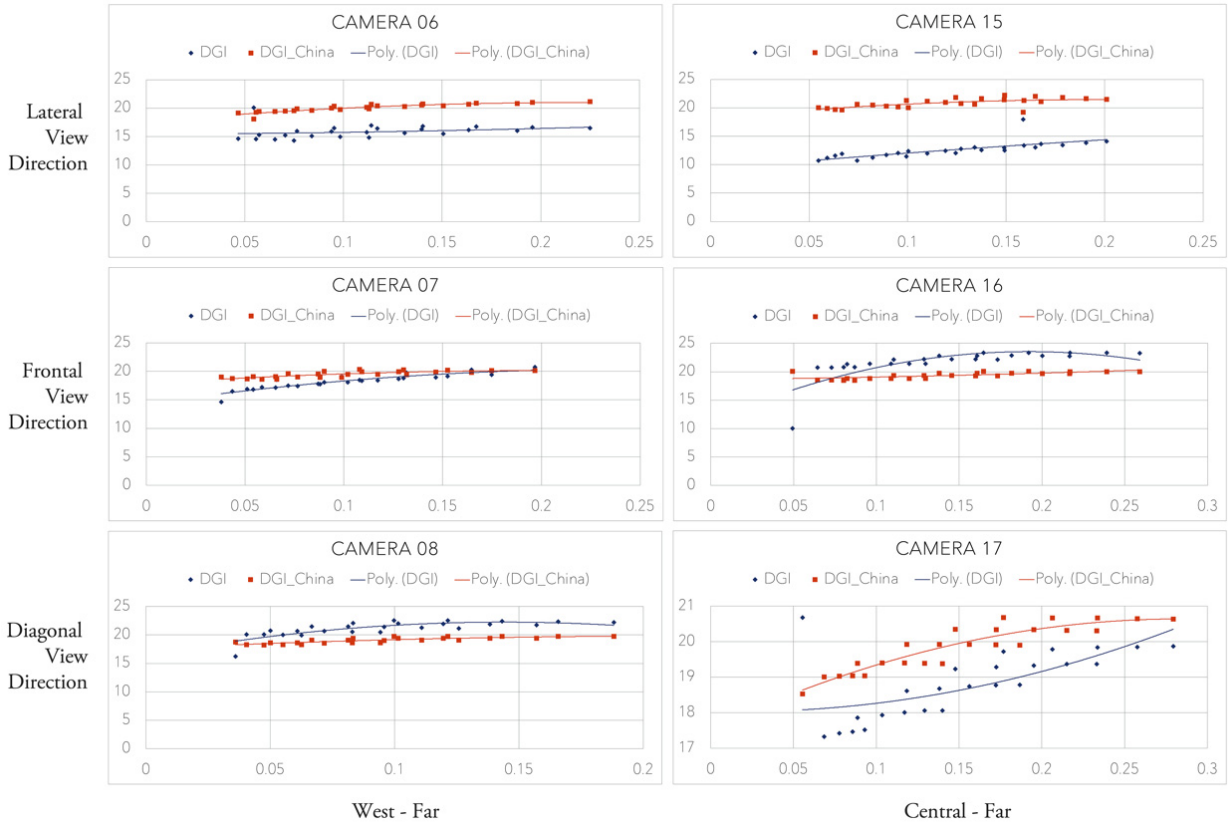

Figure 10. Comparative study on camera viewing location in the back of the room with solid angles (*X*-axis) against DGI and DGI_{China} evaluation (*Y*-axis).

As discussed above, the daylight source size calculation in DGI_{China} is based on correlating the input Radiance image with the associated building information data to identify all window pixels for the average brightness of the window, L_s. We observed that DGI_{China} significantly differs from DGI due to the modification in glare source luminance L_s to include the entire window. In many cases, DGI does not include entire windows that do not cross adaptation thresholds. This change has a more significant impact, particularly on the front viewing positions, being closest to the window and thus representing a more substantial variation in the portion of the whole Radiance image.

Whereas DGI ratings are nominally higher for views diagonally across typical office spaces (representing the view entering an office from a door in the corner) than in the middle of the same space (representing the view of a typical workstation) due to lower luminance within visual fields (a heightened "tunnel" effect), this generalization is no longer the case in DGI_{China} with the change in L_s. For instance, as shown in Figure 10, DGI_{China} results at camera positions in the back of the room, including Camera 06, Camera 07, and Camera 08, show minimum noticeable changes compared to DGI. Previous rule-of-thumb or anecdotal relationships between DGI and viewing directions or positions in buildings have been observed to change significantly in DGI_{China}.

3.3.3. Window Sizes

As shown in Figure 11, we further conduct a comparative analysis of window size impact on solid angles against DGI and DGI_{China}. In total, this study uses 25 window variations, a combination of five different window heights and five different window widths. As shown in Figures 11 and 12, DGI_{China} values from 12 selected window-to-wall ratios (WWRs) have relatively limited variations overall (no more than a range of 3 on the scale) compared to DGI. In some cases, DGI could significantly change when the window size grows above 40% of the total wall area (Figure 12). Among these variations, DGI

departs from DGI_{China} when the window size exceeds 30% of the total wall area. This discrepancy indicates that DGI_{China} is less sensitive in capturing window size variations with the consideration of the actual window geometry in the calculation.

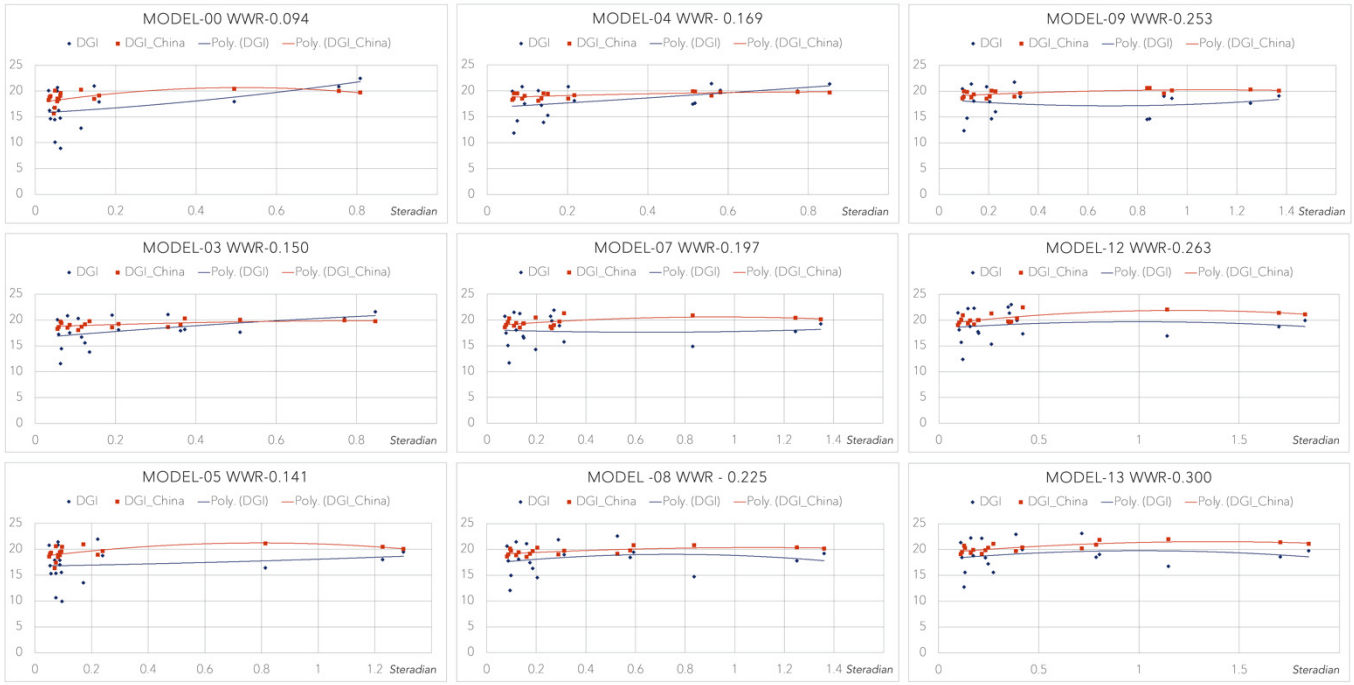

Figure 11. Comparative study on window sizes (WWR $\leq$ 0.3) with solid angles (*X*-axis) against DGI and DGI_{China} evaluation (*Y*-axis).

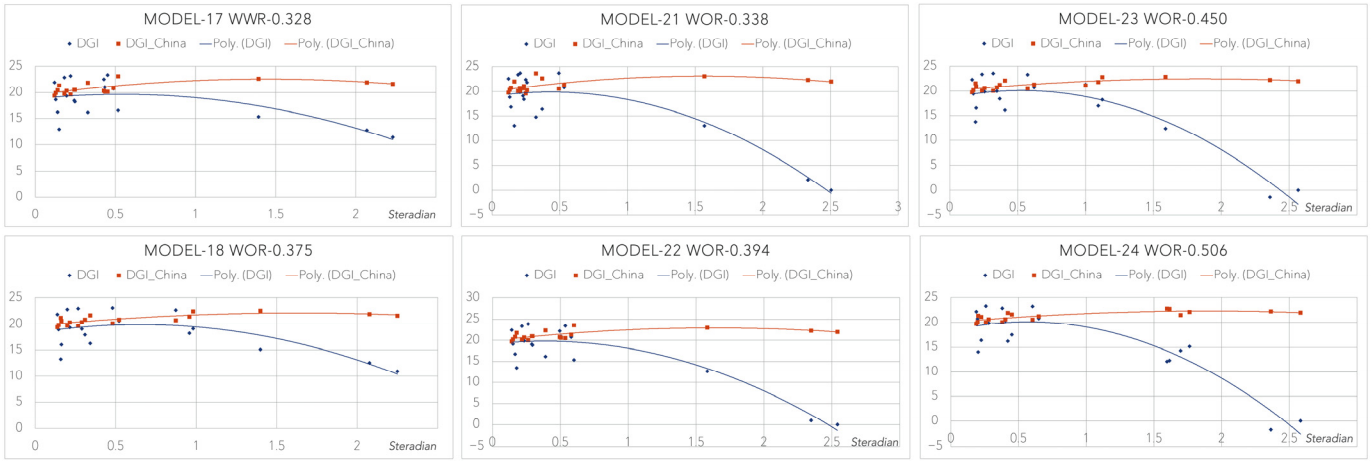

Figure 12. Comparative study on window sizes (WWR > 0.3) with solid angles (*X*-axis) against DGI and DGI_{China} evaluation (*Y*-axis).

3.4. Developing Protocols

In this section, we look into the simulation results to investigate whether representative camera positions could be chosen to recommend suitable DGI_{China} evaluation protocols. The objective is to include a minimally sufficient set of positions that would represent the glare performance of the space. The position should yield an acceptable DGI_{China} range whilst still being close to the median of possible DGI_{China} values and should not be redundant by being directly correlated to the results of another candidate position. Overall, from the 1450 simulation results, the median DGI_{China} value is 20.06. The maximum DGI_{China} value is 23.60, and the minimum DGI_{China} value 15.66. In comparison to all results grouped by camera position index (CPID), as shown in Figure 13, we found that

camera locations along the central north axis of the room have covered an upper range of the overall DGI_{China} values, in particular for the one near the window opening. Camera locations on the west side of the room better represent the median value, yet those with camera locations closest to the window cover the broadest range of the DGI_{China} values.

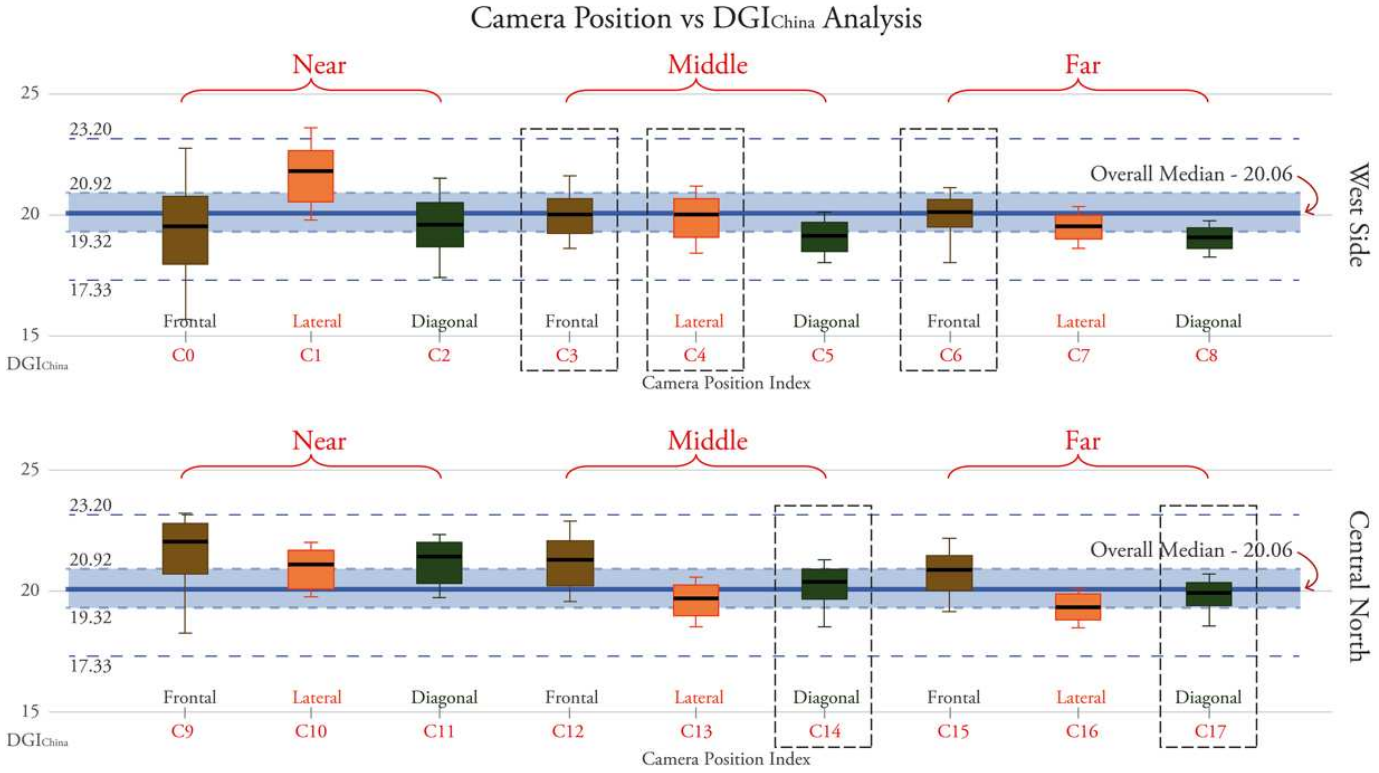

Figure 13. DGI_{China} results by Camera Position Index.

Figure 13 illustrates DGI_{China} values by Camera Position Index against the overall median value. The distribution of DGI_{China} results from each candidate position is then observed, and the distance from each group of results to the median value is then calculated and ranked. Viewing locations, including C3, C4, C6, C14, and C17 settings, are overall more representative and have close median values. It is, therefore, applicable to select only a few camera positions from these candidates to cover the representativeness of DGI_{China}. Along the central north axis of the room, the middle location of the window opening is suggested due to the overall coverage and slightly higher median value. The second recommendation will be the camera position in the middle along the west side of the room. This second camera location covers a slightly narrower range of possibilities than the far location yet has very close median values for both frontal and lateral viewing directions.

4. Discussion

4.1. Setting Standards

It is imperative when developing standards to thoroughly investigate the protocols and ensure that the standard is feasible and induces desired design changes or impacts. In the case of glare, thresholds for comfort are well accepted, as is the rule of thumb that a lower ratio between window luminance and adaptation levels lowers glare. While instituting a glare standard in China is commendable, there are not yet publicly available comprehensive studies to understand the overall implication of the standard, especially concerning the changed glare parameter, i.e., the glare source definition (L_s in Equation (2)). With a parametric evaluation workflow, we examine the positions of views in rooms as discussed in the Section 3 case study. Using large sets of simulations with representative China climatic data and reference buildings representing typical local designs and construction, we suggest the following research areas for further clarification:

- Rule sets to determine the minimally enough rooms and location of rooms in buildings with the view locations in rooms to characterize the level of glare quality in an entire building.
- Examine the effectiveness of preferred window locations and sizes in the glare standard.
- Identify cost benefits and the anticipated design impacts of DGI_{China} to the China green building standard, e.g., optimal sizes of offices for minimized glare conditions.

4.2. Departure from Established Glare Definitions

DGI_{China} departs significantly from established glare analyses in two ways: the inclusion of all visual scenarios in the metric scale and the protocols by which glare is considered. As discussed, DGI_{China} disregards the conventional definition of glare sources determined by adaptation levels and uses the average brightness of windows. This change means that windows that are not excessively bright and not considered as glare sources in established glare metrics would now yield non-zero results in DGI_{China}. In the above experiments that attempt to consider typical visual experiences in reality, we note that the *findglare* program in Radiance often omits windows that are now included in DGI_{China}. Given this fundamental difference, it can be confusing and futile to draw parallels between DGI and DGI_{China}. Moreover, with the change in the glare source definition, the window size may no longer be significant in the computation of glare, particularly when the WWR is above 30%.

Although the mean window brightness is used instead of maximum values, underestimating the likelihood of glare is very likely considering typical interior scenes that DGI_{China} is designed for and the experiments presented above attempt to consider. Considering that the view from interior spaces would typically be near the horizon (as indicated by the outer rings in Figure 14), the luminance difference across the window would not be significant.

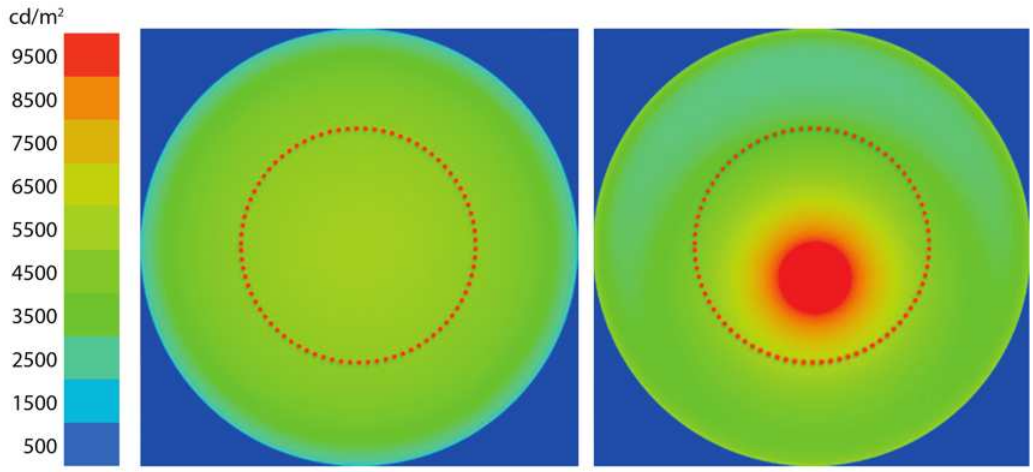

Figure 14. Shanghai Sky luminance distribution (China Standard Sky left, CIE Clear Sky right). Outer section of dashed circle denotes typical view from interior windows.

This consideration highlights the second significant departure from established analyses: the sky model protocol. Glare analyses normally assume typical and worst-case scenarios. However, as discussed earlier, the existing China standard sky model is a cloudy sky. Considering the sky luminance (left side of Figure 14) of typically visible sections to be only around 4000 cd/m^2 and window glass transmittance to be less than 0.7, the indicative brightness of windows would be less than 2800 cd/m^2, below the "Slight Perception" glare threshold in Table 2. This explains the results presented earlier that the thresholds require reexamination. As the established thresholds have empirical origins and DGI_{China} is a result of a theoretical sky model that is defined with other policy-related considerations, there is a gap between the two. It is thus necessary to re-calibrate either the scaling coefficient of DGI_{China} (0.48 in Equation (2)) or the thresholds in the DGI_{China} scale (e.g., lowering the limits).

5. Conclusions

Due to the glare source definition change from sections of sources to the entire source average brightness, the DGI_{China} glare metric requires computation not supported by prevalent glare evaluation tools. This paper, therefore, proposed a parametric modelling and simulation workflow incorporating an integrated evaluation toolkit to automate DGI_{China} calculation. Such automation demonstrates seamless support for iterative design exploration with lighting performance simulation and glare evaluation.

Besides practical ease-of-use in industry, the DGI_{China} evaluation workflow research provides complementary information for better understanding and benchmarking of the DGI_{China} stipulated thresholds, establishing appropriate protocols for its applicability, as well as directing efforts in supporting future sustainable design and evaluation in a more systematic and coherent manner.

Further research should look into the most appropriate sky model, which might not significantly affect the conclusions in this paper. Barring protocol changes in view positions and directions, the luminance values of typically visible sections highly depend on the given theoretical sky models. These would require further justifications for chosen sky models within the practical China context. For testing scenarios, further considerations should include variant sample locations in different room typologies to understand holistically how DGI in China can support glare evaluation at various design and operational stages.

Author Contributions: Conceptualization, T.-H.W. and Y.H.; methodology, T.-H.W., Y.H. and J.P.; validation, T.-H.W., Y.H. and J.P.; formal analysis, T.-H.W. and Y.H.; investigation, T.-H.W., Y.H. and J.P.; data curation, T.-H.W.; writing—original draft preparation, T.-H.W.; writing—review and editing, J.P.; visualization, T.-H.W. All authors have read and agreed to the published version of the manuscript.

Funding: This research received no external funding.

Conflicts of Interest: The authors declare no conflict of interest.

References

1. Tzempelikos, A. Advances on daylighting and visual comfort research. *Build. Environ.* **2017**, *113*, 1–4. [CrossRef]
2. Park, J.; Loftness, V.; Aziz, A.; Wang, T.H. Strategies to Achieve Optimum Visual Quality for Maximum Occupant Satisfaction: Field Study Findings in Office Buildings. *Build. Environ.* **2021**, *195*, 107458. [CrossRef]
3. Park, J.; Wang, T.H.; Witt, A.; Loftness, V. Data Acquisition and Visualization for IEQ Assessment: A case study of daylight field measurement. In Proceedings of the PLEA 2013, Munich, Germany, 10–12 September 2013.
4. Biswas, T.; Krishnamurti, R.; Wang, T.H. Framework for sustainable building design. In Proceedings of the 14th International Conference on Computer Aided Architectural Design Research in Asia, Yunlin, Taiwan, 22–25 April 2009; pp. 43–52.
5. Biswas, T.; Wang, T.H.; Krishnamurti, R. Data Sharing for Sustainable Assessments: Using functional databases for interoperating multiple building information structures. In Proceedings of the 17th International Conference on Computer Aided Architectural Design Research in Asia, Chennai, India, 25–28 April 2012; pp. 193–202.
6. Wilder, R.; Mukhopadhyay, J.; Femrite, T.; Amende, K. Evaluating glare in LEED certified buildings to inform criteria for daylighting credits. *J. Green Build.* **2019**, *14*, 57–76. [CrossRef]
7. Wasilewski, S.; Grobe, L.O.; Wienold, J.; Andersen, M. A Critical Literature Review of Spatio-Temporal Simulation Methods for Daylight Glare Assessment. *J. Sustain. Des. Appl. Res.* **2019**, *7*, 4.
8. Pierson, C.; Wienold, J.; Bodart, M. Review of Factors Influencing Discomfort Glare Perception from Daylighting: Influencing Factors. *Leukos* **2018**, *14*, 111–148. [CrossRef]
9. Quek, G.; Wienold, J.; Khanie, M.S.; Erell, E.; Kaftan, E.; Tzempelikos, A.; Konstantzos, I.; Christoffersen, J.; Kuhn, T.; Andersen, M. Comparing performance of discomfort glare metrics in high and low adaptation levels. *Build. Environ.* **2021**, *206*, 108335. [CrossRef]
10. Suk, J.; Schiler, M.; Kensek, K. Development of new daylight glare analysis methodology using absolute glare factor and relative glare factor. *Energy Build.* **2013**, *64*, 113–122. [CrossRef]
11. Hamedani, Z.; Solgi, E.; Hine, T.; Skates, H.; Isoardi, G.; Fernando, R. Lighting for work: A study of the relationships among discomfort glare, physiological responses and visual performance. *Build. Environ.* **2020**, *167*, 106478. [CrossRef]
12. Hirning, M.; Isoardi, G.; Cowling, I. Discomfort glare in open plan green buildings. *Energy Build.* **2014**, *70*, 427–440. [CrossRef]
13. Osterhaus, W. Discomfort glare assessment and prevention for daylight applications in office environments. *Sol. Energy* **2005**, *79*, 140–158. [CrossRef]

14. Lam, K.P.; Huang, Y.C.; Dobbs, G. Development of a Lighting Simulation Tool for Integrated Building Design. In Proceedings of the First International Conference on Building Energy and Environment, Dalian, China, 13–16 July 2008.
15. Park, J.; Loftness, V.; Aziz, A.; Wang, T.H. Critical factors and thresholds for user satisfaction on air quality in office environments. *Build. Environ.* **2019**, *164*, 106310. [CrossRef]
16. Park, J.; Loftness, V.; Wang, T.H. Examining In Situ Acoustic Conditions for Enhanced Occupant Satisfaction in Contemporary Offices. *Buildings* **2022**, *12*, 1305. [CrossRef]
17. Wang, T.-H.; Park, J.; Witt, A. Integrated Indoor Environmental Quality Assessment Methods for Occupant Comfort and Productivity. In Proceedings of the International Conference on Cleantech for Smart Cities & Buildings from Nano to Urban Scale, Lausanne, Switzerland, 4–6 September 2013; pp. 487–492.
18. Wienold, J.; Iwata, T.; Sarey Khanie, M.; Erell, E.; Kaftan, E.; Rodriguez, R.; Yamin Garreton, J.; Tzempelikos, T.; Konstantzos, I.; Christoffersen, J.; et al. Cross-validation and robustness of daylight glare metrics. *Light. Res. Technol.* **2019**, *51*, 983–1013. [CrossRef]
19. USGBC, LEED Reference Guide for Building Design and Construction 2020. Available online: https://www.usgbc.org/resources/leed-reference-guide-building-design-and-construction (accessed on 18 October 2022).
20. IWBI, The WELL Building Standard v2. Available online: https://www.wellcertified.com/certification/v2/ (accessed on 18 October 2022).
21. BREEAM-BRE Environmental Assessment Method. Available online: https://bregroup.com/products/breeam/ (accessed on 18 October 2022).
22. *GB/T 50378-2019*; Assessment Standard for Green Building. Ministry of Housing and Urban-Rural Development of the People's Republic of China (MOHURD): Beijing, China, 2019. Available online: https://www.codeofchina.com/standard/GBT50378-2019.html (accessed on 18 October 2022).
23. Hopkinson, R.G. Evaluation of Glare. *Illum. Eng.* **1957**, *52*, 305–316.
24. Hopkinson, R.G. Glare from daylighting in buildings. *Appl. Ergon.* **1972**, *3*, 206–215. [CrossRef]
25. Wienold, J.; Christoffersen, J. Evaluation Methods and Development of a New Glare Prediction Model for Daylight Environments with the Use of CCD Cameras. *Energy Build.* **2006**, *38*, 743–757. [CrossRef]
26. Eble-Hankins, M.L.; Waters, C.E. VCP and UGR Glare Evaluation Systems: A Look Back and a Way Forward. *Leukos J. Illum. Eng. Soc. N. Am.* **2004**, *1*, 7–38. [CrossRef]
27. Guth, S.K. A method for the evaluation of discomfort glare. *Illum. Eng. Soc.* **1963**, *58*, 351–364.
28. Guth, S.K. Computing visual comfort ratings for a specific interior lighting installation. *Illum. Eng. Soc.* **1966**, *61*, 634–642.
29. Levin, R.E. An evaluation of VCP calculations. *Illum. Eng. Soc.* **1973**, *2*, 355–361.
30. DiLaura, D.L. On the computation of visual comfort probability. *Illum. Eng. Soc.* **1976**, *5*, 207–217. [CrossRef]
31. Petherbridge, P.; Hopkinson, R.G. Discomfort Glare and the Lighting of Buildings. *Trans. Illum. Eng. Soc.* **1950**, *15*, 39–79. [CrossRef]
32. Hopkinson, R.G.; Collins, W.M. An Experimental Study of the Glare from a Luminous Ceiling. *Trans. Illum. Eng. Soc.* **1963**, *28*, 142–148. [CrossRef]
33. Einhorn, H.D. A new method for the assessment of discomfort glare. *Light. Res. Technol.* **1969**, *1*, 235–247. [CrossRef]
34. Zomorodian, Z.S.; Tahsildoost, M. Assessing the effectiveness of dynamic metrics in predicting daylight availability and visual comfort in classrooms. *Renew. Energy* **2019**, *134*, 669–680. [CrossRef]
35. Wagdy, A.; Garcia-Hansen, V.; Isoardi, G.; Pham, K. A parametric method for remapping and calibrating fisheye images for glare analysis. *Buildings* **2019**, *9*, 219. [CrossRef]
36. Suk, J.Y. Luminance and vertical eye illuminance thresholds for occupants' visual comfort in daylit office environments. *Build. Environ.* **2019**, *148*, 107–115. [CrossRef]
37. *GB 50033-2013*; Standard for Daylighting Design of Buildings. Ministry of Housing and Urban-Rural Development of the People's Republic of China (MOHURD): Beijing, China, 2013. Available online: https://www.codeofchina.com/standard/GB50033-2013.html (accessed on 18 October 2022).
38. Huang, Y.; Wang, T. Automatic Calculation of A New China Glare Index. In Proceedings of the 3rd IBPSA-England Conference: BSO 2016, Newcastle, UK, 12 September 2016; p. 1010.
39. Ward, G.W. Real Pixels. In *Graphic Gems II*; Academic Press: Cambridge, MA, USA, 1991; pp. 80–83.
40. Ward, G.W. Radiance Visual Comfort Calculation. Available online: http://radsite.lbl.gov/radiance/refer/Notes/glare.html (accessed on 18 October 2022).